International Journal of Hybrid Information Technology
Vol. 9, No.8 (2016), pp. 173-186
http://dx.doi.org/10.14257/ijhit.2016.9.8.16

Design and Implementation of an AHRS Based on Gauss Newton and Complementary Filtering Algorithm

ZhiMin Liu[1,2], Zhao Kai Ning[1], Feng Tian[1] and ZhenYue Pang[2],

1. School of Automation, Shenyang Aerospace University, Shenyang 110136, China
NZhkai@126.com
2. Shenyang Aircraft Design Institute,Shenyang, 110035,China
LZMUAV@163.com

Abstract

This paper presents design and implementation of an attitude and heading reference system (AHRS) based on Gauss Newton and Complementary Filtering algorithm (CF). The algorithm uses data measured from the MEMS sensor which contains a three-axis magnetometer, a three-axis angular rate sensor, and a three-axis accelerometer. The filter represents rotations using quaternions rather than Euler angles, which eliminates the long-standing problem of singularities associated with attitude estimation. A process model for rigid body angular motions and angular rate measurements is defined. The process model converts angular rates into quaternion rates, which are integrated to obtain quaternions. The Gauss-Newton iteration algorithm is utilized to find the optimal quaternion that relates the measured accelerations and earth magnetic field in the body coordinate frame to calculated values in the earth coordinate frame. Then fuse the optimal quaternion with the quaternion updated from gyroscope and calculate the attitude angle based on the complementary filtering algorithm . Extensive testing of the filter have proved feasibility and acceptable performance of this AHRS design.

Keywords: *Gauss-Newton Iteration Algorithm, Complementary Filtering, AHRS*

1. Introduction

Attitude and Heading Reference Systems (AHRS) are broadly applied in many fields, such as general aviation, unmanned aerial vehicle, intelligent robot and so on. The fundamental requirements for such measurement system are light weight, small size, low power consumption, and easy implementation. With the recent proliferation of micro inertial sensors based on micro-electromechanical system (MEMS) technology, it has become viable to construct inexpensive and small-size attitude measurement system. Inertial measurement unit is usually composed of three-axis gyroscopes，three-axis accelerometers and three-axis magnetometer, IMU and an online processor together often referred to as the attitude and heading reference system (AHRS). AHRS can provide the pitch angle and roll angle relative to the earth's gravity vector; and the yaw angle relative to the north [1-3].

However, due to the presence of a larger sensor measurement errors and noise, they cannot provide accurate measurements alone. In a short span of time, attitude can be estimated from integration of gyroscopes rates which tracks the attitude changes closely 00. Nevertheless, minimal errors from rotation rates will get integrated into an enormous error of the rotation angle as time elapses. However, the gyro can avoid the linear perturbation to a great extent, so it is suitable for short time attitude estimation. MEMS accelerometers together with magnetometers offer accurate attitude and heading estimation of static carriers but are sensitive to inertial forces, vibrations, or magnetic

ISSN: 1738-9968 IJHIT
Copyright © 2016 SERSC

noises. It is easy to see that frequency characteristics of these two estimations are complementary to each other and would compensate for the other's weakness. Accelerometers together with magnetometers suitable for static estimation, and gyroscope for dynamic estimation. Integration from gyroscopes tracks attitude changes closely and quickly, while observation from accelerometers and magnetometers corrects accumulated error of gyroscopes and makes the attitude and heading estimation continuously convergent 00.

So we should select an optimal online data fusion strategy to fuse the multi sensors data. The two methods that are commonly used are Extended Kalman Filtering (EKF) or some form of constant gain state observer, often termed a complementary filter due to its frequency filtering properties for linear systems. The two methods that are commonly used are Extended Kalman Filtering (EKF) or some form of constant gain state observer, often called a complementary filter due to its frequency filtering properties for linear systems. EKF is the most widely used filtering method for nonlinear system and has been studied for a range of aerospace applications. The literature 0-0 applied EKF in UAV AHRS. Such filters, however, are computationally demanding and difficult to apply robustly 00. Due to the complementary filter has the advantages of simple principle, small computationally demanding, so In practice, many applications use simple linear single-input single-output (SISO) complementary filters 00-13].

This paper presents design and implementation of an attitude and heading reference system (AHRS) based on Gauss Newton and Complementary Filtering algorithm (CF).We completed the design of AHRS hardware platform based on MEMS sensor and the design of the complementary filtering algorithm of Gauss Newton iterative algorithm 0 based on the sensor data collected by AHRS system. To test the effect of algorithm and measurement accuracy of AHRS, the output results of the AHRS system are compared with IG-500N (the AHRS commercial products made in French SBG company), finally verified the validity and accuracy of the algorithm.

2. General Hardware Architecture of AHRS

Hardware architecture of AHRS is shown in Figure 1. The IMU used in the AHRS is composed of three single axis angular rate output sensor ADXRS646，two pieces of dual axis accelerometers ADW22293 and one 3-axis MEMS magnetometers HMC5883L. This inertial unit provides measurements of linear accelerations, angular rates, and the Earth's magnetic fields for each body axis. Table 1 summarizes the basic specifications of each sensor. The main processor using an ARM architecture processor LPC1769. The IMU gets access to the sensor data of each axes into ADC7689, which are 8-channel, 16-bit, high-precision analog-to-digital converters (ADCs).The ADCs connected with MCU through SPI (Serial Peripheral Interface). Optimal attitude and heading estimation output can be delivered through an USART (Universal Synchronous/Asynchronous Receiver/Transmitter) port connect to a monitoring PC or other application devices, the communication rate up to 100 Hz.

 Copyright © 2016 SERSC

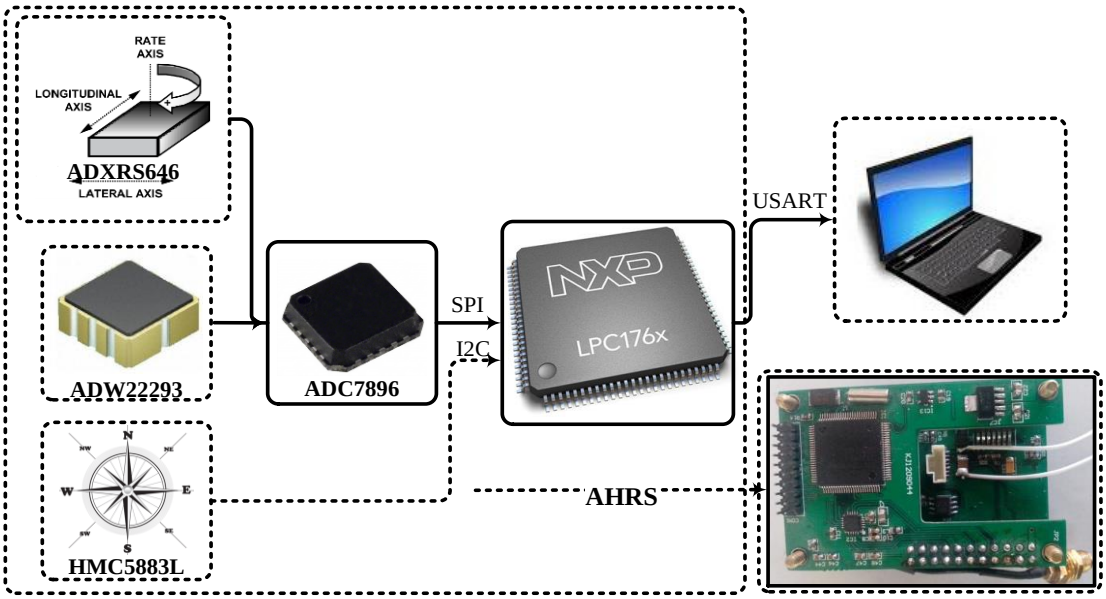

Figure 1. Hardware Architecture of AHRS

Table 1. The Basic Specifications of Each Sensor

Parameters	Gyro	Accelerometer	Magnetometer
Range	±300(sec)	±18g	±8gauss
Sensitivity	0.01(°/sec/LSB)	100mv/g	0.5(mgauss/LSB)
Bias Stability	12°/hr	-	-

3. Mathematical Background of Attitude Estimation

3.1. The Definition of Coordinate

The Euler angles describe the aircraft body-axis orientation in North, East, and down coordinates, which is Navigation coordinate (n-coordinate). The data acquired from IMU was defined in the body coordinate (b-coordinate). Here, θ is the pitch angle, φ the roll angle, and ψ is the yaw angle; as illustrated in Figure 2.

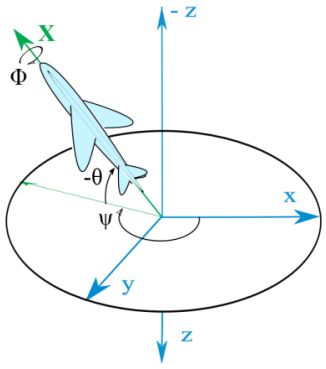

Figure 2. The Definition of Coordinates and Euler angle

3.2. AHRS Kinematic Model

The angular velocity vector expressed in body frame is ω_x for the roll rate, ω_y is the pitch rate, and ω_z is the yaw rate, and According to differential equations of Euler angles given as equation (1).

$$\begin{bmatrix} \dot{\phi} \\ \dot{\theta} \\ \dot{\psi} \end{bmatrix} = \begin{bmatrix} 1 & \tan\theta\sin\phi & \tan\theta\cos\phi \\ 0 & \cos\phi & -\sin\phi \\ 0 & \dfrac{\sin\phi}{\cos\theta} & \dfrac{\cos\phi}{\cos\theta} \end{bmatrix} \begin{bmatrix} \omega_x \\ \omega_y \\ \omega_z \end{bmatrix} \tag{1}$$

Integrating equation (1) gives numerical instability and could be gimbal locked. For this reason, a quaternion formulation to represent the attitude is preferred. Quaternions are mathematically denoted as (2), where the quaternion norm is 1.

$$q = q_0 + q_1 i + q_2 j + q_3 k, \sum_{i=0}^{3} q_i^2 = 1 \tag{2}$$

The quaternions can be represented by Euler angle as(3), where $\phi' = \frac{\phi}{2}, \theta' = \frac{\theta}{2}, \psi = \frac{\psi'}{2}$ 0.

$$\begin{aligned} q_0 &= \cos\phi'\cos\theta'\cos\psi' + \sin\phi'\sin\theta'\sin\psi' \\ q_1 &= \sin\phi'\cos\theta'\cos\psi' - \cos\phi'\sin\theta'\sin\psi' \\ q_2 &= \cos\phi'\sin\theta'\cos\psi' + \sin\phi'\cos\theta'\sin\psi' \\ q_3 &= \cos\phi'\cos\theta'\cos\psi' - \sin\phi'\sin\theta'\cos\psi' \end{aligned} \tag{3}$$

The kinematics equation (1) can be rewritten using quaternion components as (4) 0.

$$\dot{q}_t = \frac{1}{2} \cdot \omega_t \otimes q_t \tag{4}$$

$$\begin{bmatrix} \dot{q}_0 \\ \dot{q}_1 \\ \dot{q}_2 \\ \dot{q}_3 \end{bmatrix} = \frac{1}{2} \begin{bmatrix} 0 & -\omega_x & -\omega_y & -\omega_z \\ \omega_x & 0 & \omega_z & -\omega_y \\ \omega_y & -\omega_z & 0 & \omega_x \\ \omega_z & \omega_y & -\omega_x & 0 \end{bmatrix} \begin{bmatrix} q_0 \\ q_1 \\ q_2 \\ q_3 \end{bmatrix} \tag{5}$$

Additionally, the Direction Cosine Matrix(DCM) can be represented using quaternion as(6)0.

$$C_n^b = \begin{bmatrix} C_1 & 2(q_1q_2 + q_0q_3) & 2(q_1q_3 - q_0q_2) \\ 2(q_1q_2 - q_0q_3) & C_2 & 2(q_2q_3 + q_0q_1) \\ 2(q_1q_3 + q_0q_2) & 2(q_2q_3 - q_0q_1) & C_3 \end{bmatrix} \tag{6}$$

$$C_n^b = \left(C_b^n\right)^T \tag{7}$$

Where $C_1 = q_0^2 + q_1^2 - q_2^2 - q_3^2$, $C_2 = q_0^2 - q_1^2 + q_2^2 - q_3^2$, $C_3 = q_0^2 - q_1^2 - q_2^2 + q_3^2$; C_n^b represents a transformation matrix from n-coordinate to b-coordinate ; C_b^n represents a transformation matrix from b-coordinate to n-coordinate they are transposed each other.

Then, the Euler angle can be represented using quaternion as(8) 0.

 Copyright © 2016 SERSC

$$\begin{aligned}\theta &= -\arcsin\left(2\left(q_1q_3 - q_0q_2\right)\right)\\ \phi &= a\tan 2\left(\frac{2\left(q_2q_3 + q_0q_1\right)}{q_0^2 - q_1^2 - q_2^2 + q_3^2}\right)\\ \psi &= a\tan 2\left(\frac{2\left(q_1q_2 + q_0q_3\right)}{q_0^2 + q_1^2 - q_2^2 - q_3^2}\right)\end{aligned} \tag{8}$$

Where $a\tan 2$ is the four-quadrant version of the inverse tangent function, and $\arcsin$ is the arcsine function.

4. Sensor Data Fusion

The gyroscope is easily interfered by carrier vibration and impact measurement accuracy, the integrated angle drifts with time. In order to obtain more accurate attitude, needs to use the accelerometer and magnetometer measurement data to compensate the gyroscope. Usually, pitch and roll are compensated use the accelerometer data , while yaw compensated use magnetometer data. So this paper uses the Gauss-Newton iteration algorithm to find the best matched quaternion for each measurement from the accelerometers and magnetometers. The computed quaternion from the Gauss-Newton iteration algorithm is taken as part of measurements for the Complementary Filter, in addition to the measurements provided by the angular rate sensor.

4.1. Observation Estimation Based on Gauss-Newton Method

Since there are several sources of errors, As a result, there is not a quaternion that exactly converts what is measured (body frame) into the known values (earth frame). The solution is to determine the best quaternion such that, after the conversion, the error is minimized.

Equation (9) is a 6x1 vector with the measurements of gravity and magnetic field in the body frame. Equation (10) is a 6x1 vector with values of gravity and magnetic field in the earth frame. where, g is gravity of a given geographic area; b_x is the magnetic vector of x -axis; b_z is the magnetic vector of z -axis. Meanwhile, The Magnetic distortion compensation calibration models, which are further explained in Section 4.2.

$$^{b}z_t = \left[A_x(t) \quad A_y(t) \quad A_z(t) \quad M_x(t) \quad M_y(t) \quad M_z(t)\right]^T \tag{9}$$

$$^{n}z_0 = \left[0 \quad 0 \quad g \quad b_x \quad 0 \quad b_z\right]^T \tag{10}$$

The measurement error ε can be expressed as(11).

$$\varepsilon = {}^{n}z_0 - C_b^n \cdot {}^{b}z_t \tag{11}$$

Where C_b^n is the Direction Cosine Matrix (DCM) at the current time as equation(6) . Since we are considering two contributions to orientation estimation, provided by accelerometer and magnetometer, ε computation must be rewritten as(12)。

$$\varepsilon = {}^{n}z_0 - M_t\,{}^{b}z_t \tag{12}$$

$$M_t = \begin{bmatrix} C_b^n & 0 \\ 0 & C_b^n \end{bmatrix} \tag{13}$$

Let f be the error function defined as (14)[15].

$$f = \varepsilon^T\varepsilon = \left({}^{n}z_0 - M_t\,{}^{b}z_t\right)^T\left({}^{n}z_0 - M_t\,{}^{b}z_t\right) \tag{14}$$

Copyright © 2016 SERSC

Because ${}^{b}z_t$ is measured and ${}^{n}z_0$ is known, the error between them is a function of the matrix M_t, which in turn depends on the four components of the quaternion. The objective is to find iteratively the values of quaternion components that yield the minimum error. Gauss-Newton algorithms is one of the most used optimization algorithms which only use the first derivative (Jacobian), which is related to the gradient. For the Gauss-Newton method it is given as (15):

$$\hat{X}_{k+1} = \hat{X}_k - \left[J^T(\hat{q}_k) \cdot J(\hat{q}_k) \right]^{-1} \cdot J^T(\hat{q}_k) \cdot \varepsilon(\hat{q}_k) \tag{15}$$

where $\hat{q}_k$ is a vector with the four components of the quaternion and J is the Jacobian matrix defined as (16). After performing the derivatives and matrix products, the Jacobian matrix can be rewritten as follows(17):

$$\begin{aligned} J_k(\hat{q}_k(t)) = & \\ & \begin{bmatrix} 2(q_0A_x - q_3A_y + q_2A_z) & 2(q_1A_x + q_2A_y + q_3A_z) \\ 2(q_3A_x + q_0A_y - q_1A_z) & 2(q_2A_x - q_1A_y - q_0A_z) \\ 2(-q_2A_x + q_1A_y + q_0A_z) & 2(q_3A_x + q_0A_y - q_1A_z) \\ 2(q_0M_x - q_3M_y + q_2M_z) & 2(q_1M_x + q_2M_y + q_3M_z) \\ 2(q_3M_x + q_0M_y - q_1M_z) & 2(q_2M_x - q_1M_y - q_0M_z) \\ 2(-q_2M_x + q_1M_y + q_0M_z) & 2(q_3M_x + q_0M_y - q_1M_z) \end{bmatrix} \\ & \begin{bmatrix} 2(-q_2A_x + q_1A_y + q_0A_z) & 2(-q_3A_x - q_0A_y + q_1A_z) \\ 2(q_1A_x + q_2A_y + q_3A_z) & 2(q_0A_x - q_3A_y + q_2A_z) \\ 2(-q_0A_x + q_3A_y - q_2A_z) & 2(q_1A_x + q_2A_y + q_3A_z) \\ 2(-q_2M_x + q_1M_y + q_0M_z) & 2(-q_3M_x - q_0M_y + q_1M_z) \\ 2(q_1M_x + q_2M_y + q_3M_z) & 2(q_0M_x - q_3M_y + q_2M_z) \\ 2(-q_0M_x + q_3M_y - q_2M_z) & 2(q_1M_x + q_2M_y + q_3M_z) \end{bmatrix} \end{aligned} \tag{16}$$

$$\begin{aligned} J_t(\hat{q}_k(t)) = \frac{d(\varepsilon)}{dq_k(t)} = -\Bigg[& \left(\frac{dM}{dq_0} \cdot {}^{b}z_t \right) \left(\frac{dM}{dq_1} \cdot {}^{b}z_t \right) \\ & \left(\frac{dM}{dq_2} \cdot {}^{b}z_t \right) \left(\frac{dM}{dq_3} \cdot {}^{b}z_t \right) \Bigg] \end{aligned} \tag{17}$$

Note that the quaternion vector $\hat{q}_k(t)$ refers to the k-th iteration at the current time t (during each time an acquisition from the IMU is performed, and more than one iteration per time could be computed, in order to faster reach the minimum point).Finally, the next iteration quaternion is computed as follows:

$$\begin{aligned} \hat{q}_{k+1}(t) = \hat{q}_k(t) - & \left[J_t(\hat{q}_k(t))^T \cdot J_t(\hat{q}_k(t)) \right]^{-1} \cdot \\ & J_t(\hat{q}_k(t))^T \left(z_0 - M_t(\hat{q}_k) \cdot z_t \right) \end{aligned} \tag{18}$$

The feasibility of this approach heavily relies on fast convergence of the Gauss-Newton iteration algorithm. Extensive simulations show that the iteration algorithm converges in just 3 to 4 steps, which ensures the success of this alternative approach0.

4.2. Magnetic Distortion Compensation

 Copyright © 2016 SERSC

Measurements of the earth's magnetic field will be distorted by the presence of magnetic elements in the vicinity of the magnetometer. Investigations into the effect of magnetic distortions on magnetometer's performance have shown that substantial errors may be introduced by sources including electrical appliances, metal furniture and metal structures within a buildings construction 0. Sources of interference fixed in the sensor frame, termed hard iron biases, can be removed through calibration. Sources of interference in the earth frame, termed soft iron, cause errors in the measured direction of the earth's magnetic field. Declination errors that in the horizontal plane relative to the earth's surface, cannot be corrected without an additional reference of heading. Inclination errors that in the vertical plane relative to the earth's surface, may be compensated for as the accelerometer provides an additional measurement of the sensor's attitude. Using the latest quaternion computed, $\hat{q}(t)$, the magnetic reference in the earth frame is obtained as follows 0:

$$^{E}h_t = \begin{bmatrix} 0 & h_x & h_y & h_z \end{bmatrix} = \hat{q}(t) \otimes {}^{S}m_t \otimes \hat{q}^{*}(t) \tag{19}$$

$$^{S}m_t = \begin{bmatrix} 0 & m_t \end{bmatrix}$$

Where $\hat{q}^{*}(t)$ indicates the conjugate of $\hat{q}(t)$ and m_t is the normalized magnetometer measurements at time t. This is achieved by computing $^{E}b_t$, as $^{E}h_t$ normalized to have only components in the earth frame x and z axes; as described by equation:

$$^{E}b_t = \begin{bmatrix} b_x & 0 & b_z \end{bmatrix} = \begin{bmatrix} \sqrt{h_x^2 + h_y^2} & 0 & h_z \end{bmatrix} \tag{20}$$

Compensating for magnetic distortions in this way ensures that magnetic disturbances are limited to only affect the estimated heading component of orientation. The approach also eliminates the need for the reference direction of the earth's magnetic field to be predefined; a potential disadvantage of other orientation filter designs 0 .The architecture of Magnetic distortion compensation as Figure 3.

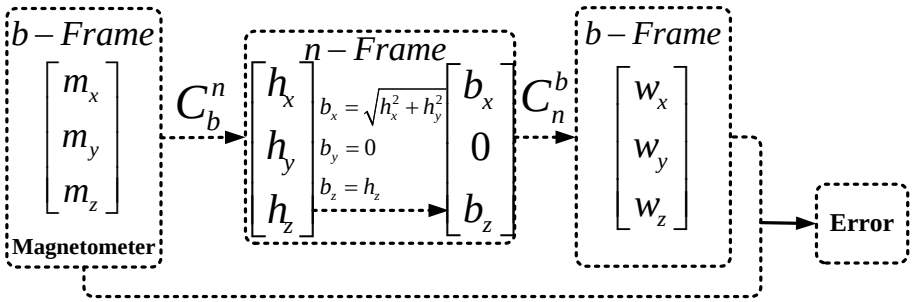

Figure 3. The Architecture of Magnetic Distortion Compensation

4.3. Quaternion Complementary Filter

Gyroscope is more accurate in dynamic situation, but the integrated angle drifts with time. Magnetometer and accelerometer measurement don't corrects accumulated error, but the dynamic response is poor. Therefore, they are combined in frequency domain, fuse the three kinds of sensor data using complementary filter, improve the accuracy of the measurement and the system dynamic performance.

The filter is derived from the complementary filtering theory 0. The general requirement is that one of the transfer functions complements the sum of the others. Thus for n measurements of a signal:

$$T_1(s) + T_2(s) + \ldots + T_{n-1}(s) + T_n(s) = 1 \tag{21}$$

Copyright © 2016 SERSC

where s is the time integration Laplace operator.Figure 4 shows the show the transform domain block diagram of the linearized quaternion Complementary Filter.

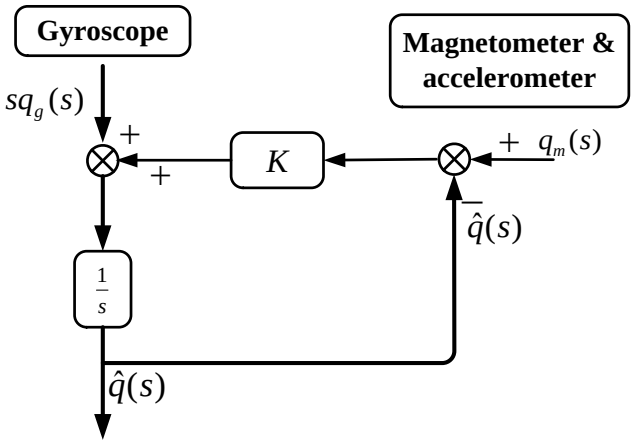

Figure 4. The Diagram of the Transform Domain (Laplace) of the Linearized Quaternion Complementary Filter

Let the Laplace transform of the quaternion q_m (obtained from accelerometer and magnetometer readings) be $q_m(s)$, while $q_g(s)$ is the quaternion obtained by integrating gyroscope signals and $sq_g(s)$ is the Laplace transform of in equation (4). Note that the accelerometer measures both gravitational and linear accelerations and the gyroscope suffers from bias. Therefore, $q_m(s)$ and $q_g(s)$ are both disturbed. From Figure 4, the filter transfer function $F_1(s)$ based on accelerometer and magnetometer inputs is given by:

$$F_1(s) = \frac{\hat{q}(s)}{q_m(s)} = \frac{C(s)s^{-1}}{1+C(s)s^{-1}} = \frac{C(s)}{s+C(s)} \tag{22}$$

Note that equation (22) has the form of first-order low-pass filter which proves that the perturbation effects due to high frequency components of accelerometer signal (linear acceleration) are filtered from. $q_m(s)$ Similarly, from equation (4), the filter transfer function based on gyroscope input can be written such as:

$$F_2(s) = \frac{\hat{q}(s)}{q_g(s)} = \frac{1}{1+C(s)s^{-1}} = \frac{s}{s+C(s)} \tag{23}$$

Note that (23) has the form of first-order high-pass filter. The gyroscope measurements are high-pass filtered with respect to the output $\hat{q}(s)$. So, the perturbations due to low frequency components of gyroscope signal (the noises and biases) are filtered from $q_g(s)$ .Finally, (21) can be verified:

$$\frac{\hat{q}(s)}{q_m(s)} + \frac{\hat{q}(s)}{q_g(s)} = \frac{C(s)}{s+C(s)} + \frac{s}{s+C(s)} = 1 \tag{24}$$

The global transfer function of the Complementary Filter is:

$$\hat{q}(s) = \left(\frac{C(s)}{s+C(s)}\right) q_m(s) + \left(\frac{s}{s+C(s)}\right) q_g(s) \tag{25}$$

One can conclude from (25) that Complementary Filter blends a low-pass filtering on the signals from the accelerometer-magnetometer pair, and a high-pass filtering on the

 Copyright © 2016 SERSC

signals from the gyroscope. From equation (4) and (21), the function can be written such as:

$$s\hat{q}(s) = C(s)(q_m(s)) - \hat{q}(s)) + \dot{q}_g(s) \tag{26}$$

If $C(s)$ is a constant K_p ,then the cut-off frequency of the Complementary Filter is $f_T = {K_p}/{2\pi}$, when the cut-off frequency is larger than f_T, gyroscope plays the main role for the estimate result; when the cut-off frequency is lower than f_T, accelerometer and magnetometer plays the main role for the estimate result. In order to eliminate the static error， let $C(s) = K_p + {K_i}/{s}$,the cut-off frequency of complementary filter was decided by the value of K_p, the time of eliminate static deviation was decided by the value of K_i. Generally, the value of K_i is 0.01～0.1 times of K_p. The chosen value for K_p has been 0.98, as in 0.

The diagram of complete attitude estimate algorithm based on Gauss Newton and Complementary Filtering algorithm is shown in Figure 5. Group 1 is magnetic distortion ; Group 2 is the architecture of Gauss Newton iteration algorithm. Group 3 is the basic structure of Complementary filter algorithm.

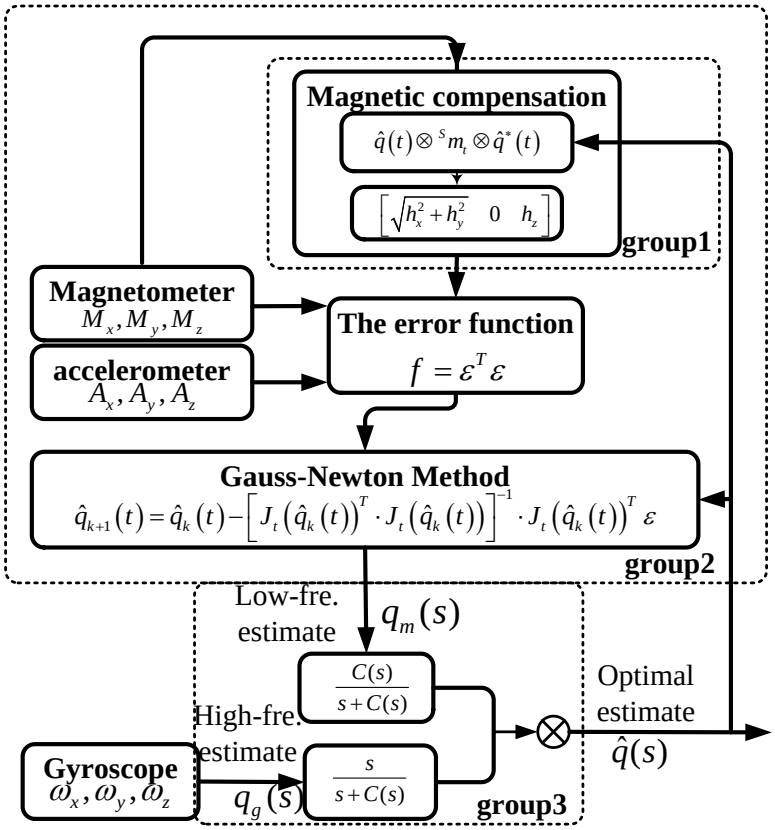

Figure 5. The Diagram of Complete Attitude Estimate Algorithm Based on Gauss- Newton and Complementary Filtering Algorithm

Copyright © 2016 SERSC

5. Experiment Result

In order to make the AHRS output visible, we coded a monitoring program based on Windows MFC and OpenGL that can real time display Euler angles, gyro rates, and accelerometer and magnetometer measurements simultaneously. The data acquisition was performed through a RS-232 communication serial port and the measurement data can be saved as an excel file for further simulation analysis. Figure 6 introduces architecture of the AHRS monitoring system.

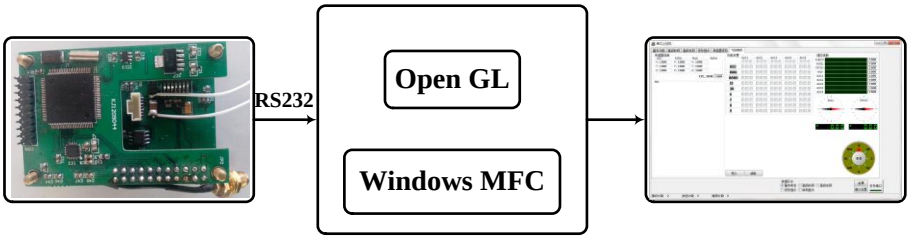

Figure 6. The Architecture of the AHRS Monitoring System

Further validating the AHRS performance, using the output of IG-500N (the AHRS commercial products made in French SBG company) as the reference value(the sampling frequency is 100Hz), and verify the complementary filtering algorithm using MATALB. This product is composed of the IMU based on MEMS sensors, the GPS receiver and the pressure sensor, and embedded with the extended Kalman data fusion algorithm can provide high precision 3D attitude data. We fixed both AHRS on the same carrier and the data was obtained for a sequence of rotations performed by hand. The measurements of accelerations $\begin{bmatrix} A_x & A_y & A_z \end{bmatrix}$,angular rates $\begin{bmatrix} \omega_x & \omega_y & \omega_z \end{bmatrix}$ and magnetic fields $\begin{bmatrix} m_x & m_y & m_z \end{bmatrix}$, during the test are shown in Figure 7.

Copyright © 2016 SERSC

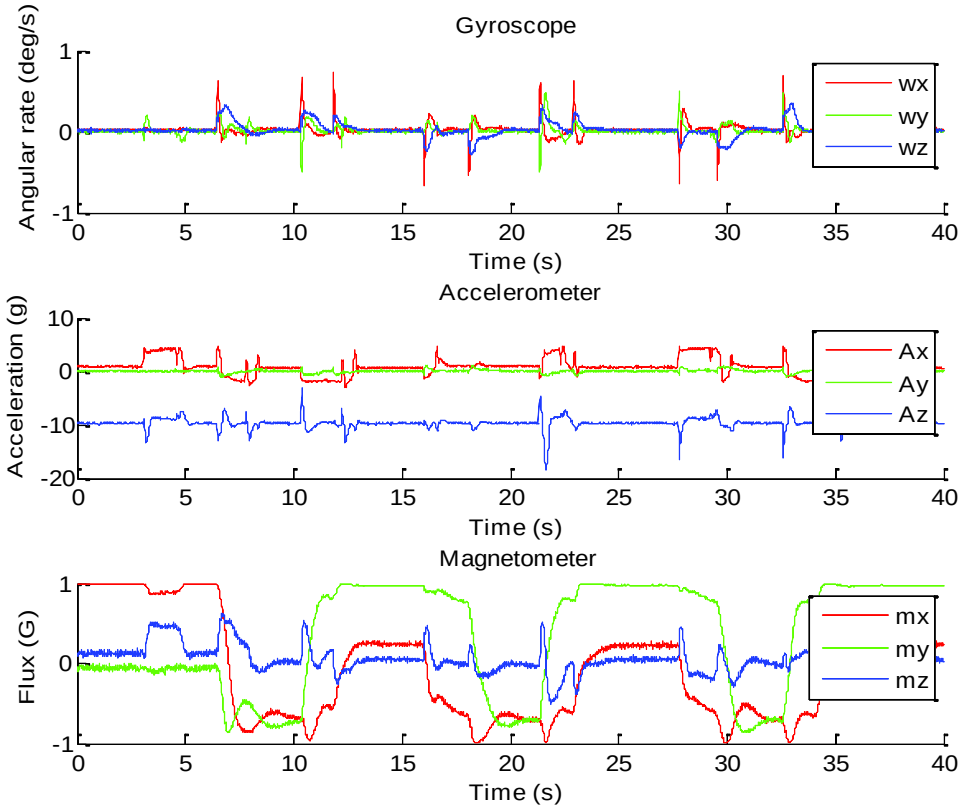

Figure 7. Raw Data from AHRS

The measurements of MEMS inertial and magnetic sensors output obtained during the experimental test are used for the implementation of the attitude estimation. The time responses for roll, pitch, and yaw are plotted in Figure 8. Where, the dotted line represents the output of the estimate attitude and the solid line represents the output of IG-500N。 The error between reference and filtering is provided in Figure 9.

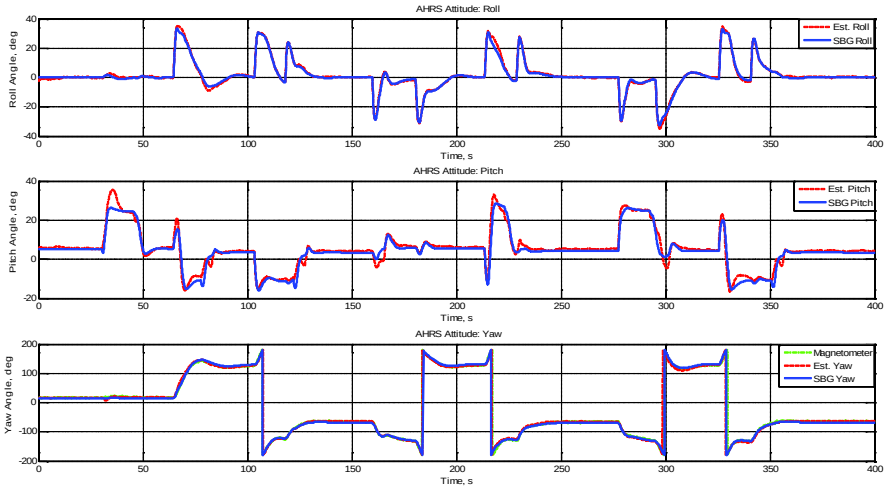

Figure 8. Output Comparisons of Pitch, Roll and Yaw

Copyright © 2016 SERSC

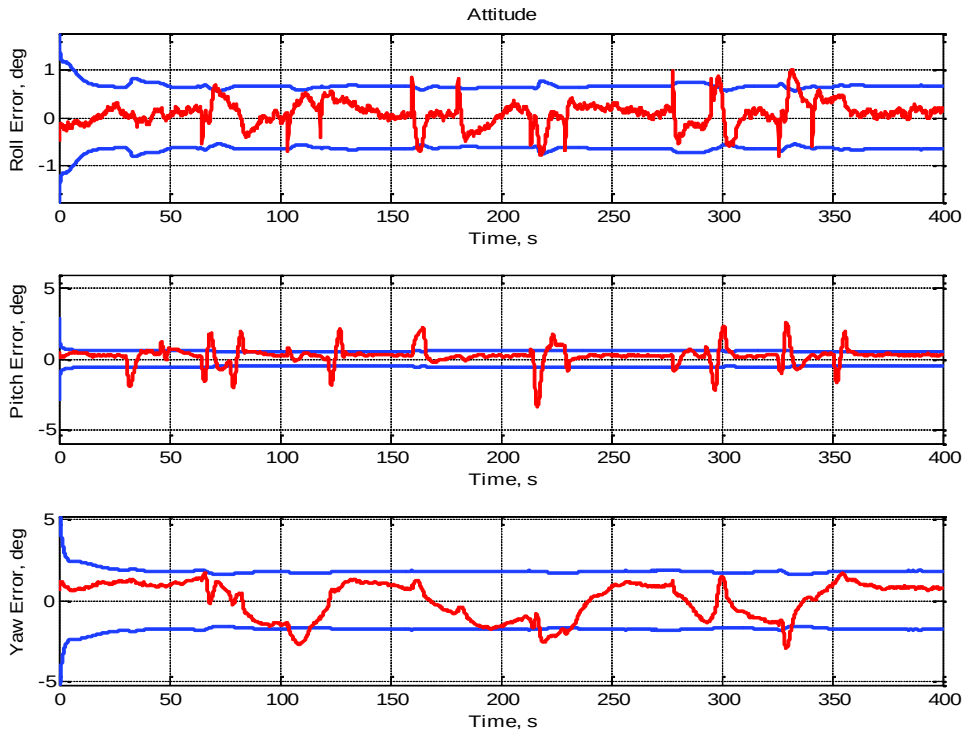

Figure 9. The Error between Reference and Filtering

In order to verify the effectiveness of the estimation, the root mean square (RMS) of the attitude error are calculated to quantify the estimate performance. The RMS are 0.5214, 0.7720, 2.0788 degree for roll, pitch, and heading, respectively. The RMS error of AHRS are shown in Table 2. The test results shows that the estimation error remained in the ± 2 deg and proves feasibility, stableness, and accuracy of the AHRS based on Gauss Newton and Complementary Filtering algorithm (CF) designed in this paper.

Table 2. The RMS Error of AHRS

Euler parameter	Complementary filter
Pitch	0.5214°
Roll	0.7720°
Yaw	2.0788°

6. Conclusion

As is explained in the above sections, we have designed and implemented an AHRS with MEMS sensors based on Gauss Newton and Complementary Filtering algorithm (CF). Extensive experimental test shows that, this fusion strategies, can effectively fusion the measurement data acquired from the gyroscope, acceleration sensor and magnetometer, and the AHRS has a good response characteristics. The estimate error is remained in 2 degree, can meet the attitude control requirement of the low cost UAV.

Copyright © 2016 SERSC

References

[1] S. Chen, C. Ding and Y. Han, "Study on Information Fusion Algorithm for the Miniature AHRS. Proceedings of the 4th International Conference on Intelligent Human-Machine Systems and Cybernetics, Nanchang, China, **(2012)**.
[2] J. Rios and E. White, "Fusion Filter Algorithm Enhancements for a MEMS GPS/IMU", Proceedings of the 21th National Technical Meeting of The Institute of Navigation, San Diego, California,**(2002)**.
[3] Y. Wang, N. Li, X. Chen and M. Liu, "Design and Implementation of an AHRS Based on MEMS Sensors and Complementary Filtering", Journal Advances in Mechanical Engineering, vol. 3, no. 3, **(2014)**.
[4] A. Chan, S. Tan and C. Kwek, "Sensor data fusion for attitude stabilization in a low cost quadrotor system", Proceedings of the International Symposium on Consumer Electronics (ISCE), Singapore, **(2011)**.
[5] M. Cordero, F. Alarcn, A. Jimnez, A. Viguria and A.Ollero, "Survey on Attitude and Heading Reference Systems for Remotely Piloted Aircraft Systems", Proceedings of the International Conference on Unmanned Aircraft Systems (ICUAS), **(2014)**.
[6] R.R. Lima and L. A. B. Torres, "Performance Evaluation of Attitude Estimation Algorithms in the Design of an AHRS for Fixed Wing UAVs", Proceedings of the 1st Brazilian Robotics Symposium (SBR) and the 9th Latin American Robotics Symposium (LARS), **(2011)**.
[7] P. Martin and E. Salaun, "Design and implementation of a low-cost observer-based attitude and heading reference system", Journal Control Engineering Practice, vol. 7, no. 18, **(2010)**.
[8] M. De, G. Hector, F. Pereda, J. Giron-Sierra and E.Felipe, "UAV Attitude Estimation Using Unscented Kalman Filter and TRIAD", Journal IEEE Transactions on Industrial Electronics, vol. 11, no. 59, **(2012)**.
[9] Y. Li, E. Mahmoud, C. Anthony and G. Andrew, "Performance evaluation of AHRS Kalman filter for MojoRTK system", Proceedings of International Global Navigation Satellite Systems Society (IGNSS) Symposium, Queensland, Australia, **(2009)**.
[10] C.W. Kang and C.G. Park, "Attitude estimation with accelerometers and gyros using fuzzy tuned Kalman filter", Proceedings of the European Control Conference (ECC), Budapest, Hungary, **(2009)**.
[11] Y. Liang, M. Cheng, F. He and F. Li Hang, "Attitude estimation of a quad-rotor aircraft based on complementary filter", Journal Transducer and Microsystem Technologies, vol. 11, no. 30, **(2011)**.
[12] S. Yan, Y. Wang and H. Zhang, "Improved complementary filter for attitude estimation of micro air vehicles using low-cost inertial measurement units", J. Journal of Computer Applications, vol. 7, no. 33, **(2013)**.
[13] J. Sun, Y. You and Z. Fu, "Attitude Estimation Based on Conjugate Gradient and Complementary Filter", J. Chinese Journal of Sensors and Actuators, vol. 4, no. 27, **(2014)**.
[14] S. Madgwick, "An efficient orientation filter for inertial and inertial/magnetic sensor arrays", J. Report x-io and University of Bristol (UK), **(2010)**.
[15] J. Marins, X. Yun, E. Bachmann, R. McGhee and M. Zyda, "An Extended Kalman Filter for Quaternion-Based Orientation Estimation Using MARG Sensors", Proceedings of the IEEE International Conference on Intelligent Robots and Systems, Maui, HI, United states, **(2001)**.
[16] W. H. K. De Vries, H. E. J. Veeger, C. T. M. Baten and F. C. T. Van Der Helm, "Magnetic distortion in motion labs", implications for validating inertial magnetic sensors, Journal Gait & posture, vol. 4, no. 29, **(2009)**.
[17] A. Sabatini, "Quaternion-based extended kalman filter for determining orientation by inertial and magnetic sensing", J. IEEE Transactions on Biomedical Engineering, vol. 7, no. 53, **(2006)**.
[18] W. Higgins, "A comparison of complementary and Kalman filtering", Journal IEEE Transactions on Aerospace and Electronic Systems, vol. 3, no. 11, **(1975)**.

Authors

ZhiMin Liu, He received the master degree from Beijing University of Aeronautics and Astronautics, China. He is currently professor at the College of Automation of Shenyang Aerospace University. He is the chief technical expert of AVIC.

Copyright © 2016 SERSC

ZhaoKai Ning, He received the bachelor degree in Measurement and control technology and instrument from Qilu University of Technology, China, in 2013.He is currently studying for a master degree in the control engineering of Shenyang Aerospace University.

Copyright © 2016 SERSC